FACTA UNIVERSITATIS
Series: **Electronics and Energetics** Vol. 37, Nº 4, December 2024, pp. 619 – 637
https://doi.org/10.2298/FUEE2404619B

Original scientific paper

OPTIMIZED EEMD FEATURE EXTRACTION USING BIO-INSPIRED OPTIMIZATION ALGORITHMS FROM ELECTROCARDIOGRAM SIGNALS*

Amit Bakshi, Mamata Panigrahy, Jitendra Kumar Das

School of Electronics Engineering, KIIT Deemed to be University, Bhubaneswar, India

ORCID iDs: Amit Bakshi https://orcid.org/0000-0003-2702-3790
Mamata Panigrahy https://orcid.org/0000-0003-3686-5543
Jitendra Kumar Das https://orcid.org/0000-0003-4249-577X

Abstract. *Electrocardiogram (ECG) signal analysis is crucial for diagnosing heart conditions. The empirical Mode Decomposition (EMD) technique is quite effective in analyzing non-stationary signals. However, it has the inherent problem of mode mixing. To overcome this, the Ensemble Empirical Mode Decomposition (EEMD) method incorporates noise with known variance, utilizes the ensemble nature of EMD and enhances the decomposition process. This paper proposes a novel method for extracting features using EEMD to make its parameters independent. The intrinsic mode functions (IMFs) extracted from EEMD may vary depending on the parameters used. In contrast, EMD exhibits parameter independence, which ensures greater consistency. To obtain consistent results from EEMD without sacrificing its advantages over EMD, different bio-inspired optimization techniques have been employed. Once consistent IMFs are generated, amplitude modulation (AM) and frequency modulation (FM) signals within each IMF are distinguished. Finally, the retrieved bandwidth of the AM/FM signals is utilized as feature vectors. These features are then evaluated using two well-established classifiers like Support Vector Machine (SVM) and Decision Tree (DT). The respective classifier accuracy levels of 91% and 98.94% were achieved using published datasets. The result shows the efficiency of the proposed feature extraction techniques.*

Key words: *Intrinsic mode function, empirical mode decomposition, ensemble EMD, Support vector machines, Decision Tree*

1. INTRODUCTION

Cardiac arrhythmia causes a significant health concern worldwide, contributing to morbidity and mortality across diverse populations [1]. Timely and accurate detection of arrhythmic events is essential for effective intervention and management of cardiovascular

Received October 11, 2023; revised May 21, 2024, June 23, 2024, July 26, 2024 and August 20, 2024; accepted September 24, 2024
Corresponding author: Amit Bakshi
School of Electronics Engineering, KIIT Deemed to be University, Bhubaneswar, India
E-mail: amitfet@kiit.ac.in

diseases. Recent advances in signal processing, especially in electrocardiogram (ECG) analysis, have provided promising new paths for better cardiac arrhythmia detection and prevention. Different features are extracted from sinus-rhythm ECG and cardiac disorder ECG signals and compared to detect the abnormality. In recent decades, researchers have developed and proposed a multitude of signal processing algorithms and machine learning (ML) models to automatically analyze ECG signals for cardiac arrhythmias and abnormalities [2]. Researchers use a hybrid Deep Learning model (DL) that integrates attention mechanisms with a Convolutional Neural Network (CNN) and Long Short-Term Memory (LSTM) to categorize cardiac arrhythmias [3]. By using CNNs for feature extraction and providing the LSTM component with the most discriminative characteristics from the input, this method seeks to reduce dimensionality. R. Saravana Ram et al. [4] presented the HybDeepNet model, which uses ECG signals to detect cardiac arrhythmias. This hybrid deep learning network combines three models: Deep Belief Networks (DBNs), Multilayer Perceptrons (MLPs), and Restricted Boltzmann Machines (RBMs). While the model shows robustness, as evidenced by the obtained AUC and F1-score values, there is room for improvement in its detection performance.

Non-stationary signals are signals with time-varying statistical characteristics like variance and mean. The analysis of highly unstable signals becomes more complicated due to their great variability and unpredictability over time. Signal feature extraction with a high level of efficacy, possesses the ability to decompose signals into smaller components. Nowadays, these decomposition processes are competent enough to process highly unstable and non-stationary signals with greater precision. While early attempts at signal decomposition utilized wavelet transform, this method reliance on specific mathematical functions limits its robustness [5, 6]. In pursuit of a more adaptive approach for electrocardiogram (ECG) signal analysis, empirical mode decomposition (EMD) has emerged as a highly effective and widely accepted technique with low computational intricacy and more precise characterization in contrast with multivariate EMD for ECG signal characterization issues [7-9]. The mean frequency (MF) proportion of intrinsic mode functions (IMFs) has been utilized as a component to recognize the contrast between sinus-rhythm and cardiac disorders ECG signals [7]. The weighted frequency has been utilized as a feature of IMFs for clearly distinguishing sinus-rhythm and cardiac disorder ECG signals [6]. There are a few procedures for the examination of normal sinus rhythm and cardiac disorder ECG signals that have been proposed in [5-7], which depend on EMD growth, particularly for non-linear and non-stationary signal investigation.

The Empirical Mode Decomposition (EMD) method breaks down a signal into intrinsic mode functions (IMFs). The decomposition is achieved through an iterative procedure known as a sifting process. Each IMF can be represented with elementary AM-FM-type signals. Features like the bandwidth of these signals are utilized to detect the cardiac abnormalities in the ECG signal. The problem of mode mixing, in which various frequency components may be mixed in a single IMF, is one of the major drawbacks of EMD [7]. To address this challenge, the Ensemble Empirical Mode Decomposition (EEMD) method was introduced by Wu and Huang [10]. EEMD tries to reduce mode mixing by adding white noise to the signal over multiple trials and defining IMF components as the mean of these trials.

By repeating the process similar to EMD for each trial, the added noise can be effectively cancelled out in the ensemble mean, using an optimal number of trials determined based on recommendations in the literature [11]. With an increasing number of trials, only the original signal persists, ensuring accurate decomposition. The amplitude of the added noise denoted as

An, significantly influences the performance of the EEMD method in mode separation. An amplitude that is too low, may not induce sufficient changes in the decomposed signal, while an excessively high amplitude could result in redundant IMFs [10].

To address this issue, a perfect set of decision variables is selected to be used for optimization using established bio-inspired optimization algorithms based on some metaheuristic techniques [12]. In this bio-inspired type of optimization algorithm, the impact of decision variables on the EEMD performance is represented as a fitness function. The least value obtained is to be taken as the optimal parameter value. The metaheuristic optimization techniques are quite good in finding optimum function values from the range of decision variables considered. In addition to this, these techniques help to get excellent solutions for optimization problems, especially in cases of limited computational capacity. The simplicity, flexibility, and local optimum avoidance can be easily carried out using such techniques. Every such technique goes through two stages i.e. exploration and exploitation. In the exploration phase, it tries to identify the best possible area from the search space and the later one tries to apply local search on the promising area to improvise each individual in the search space. Even if these techniques are broadly classified as evolutionary algorithms and swarm-based algorithms, both types belong to the population-based bio-inspired algorithm. In the case of evolutionary algorithms such as genetic algorithm (GA), as individual solutions in search space whereas in the case of swarm-based methods, different types of swarms are represented as solutions in search space. There are many swarm-based optimization algorithms like particle swarm optimization (PSO), ant colony optimization (ACO), grey wolf optimization (GWO), and whale optimization algorithm (WOA). Each of the techniques has its way of updating the swarm position and hence the time to reach convergence along with converging solution depends on this updating strategy. The objective of the execution of these algorithms starts from the formation of a perfect fitness function [11-13].

In this paper, an optimized EEMD approach is proposed to make it parameter-independent for improved consistency. To retrieve the best possible decomposed signals, frequency components from the amplitude-modulated signal (B_{AM}) and frequency-modulated signal (B_{FM}) are extracted, for the classification of sinus-rhythm and cardiac disorders ECG signals.

The remainder of this paper is structured as follows: Section 2 provides an overview of the methods employed including dataset considerations, EEMD-based decomposition, and optimization techniques. Section 3 discusses the performance comparison of the proposed PSO-EEMD method with the WOA-EEMD approach and presents the result. Finally, Section 4 concludes the paper.

2. METHODS

Our study aims to identify significant features from ECG datasets. To show the robustness of the proposed methodology in a parameter-dependent environment of EEMD, we chose two publicly available and recognized databases from PhysioNet. However, obtaining perfect IMFs by EEMD is inconsistent due to its dependence on various parameters, as described later in this section. Therefore, we included optimization strategies to address this issue. The following sections describe the use of nature-inspired optimization techniques to enhance EEMD algorithms, improving their robustness and effectiveness in extracting features from ECG signals.

2.1. Dataset

In this work, we have used binary class datasets from PhysioNet for classification tasks. These datasets have proven essential in the study of signal classification using the application of advanced machine learning models [14]. Signal variations, which are considered features, correspond to electrocardiogram (ECG) patterns of sinus-rhythm heartbeats as well as those affected by various arrhythmias and myocardial infarction. Pre-processing and segmentation techniques were applied to these signals to create segments that correspond to each heartbeat.

The datasets used in our work are:

MIT-BIH Arrhythmia Database: This dataset includes ECG recordings from 47 different subjects, sampled at 360 Hz with 11-bit resolution. At least two cardiologists annotate each beat according to the Association for the Advancement of Medical Instrumentation (AAMI) EC57 standard [15]. The categories include "normal beat (N)," "supra-ventricular premature beat (S)," "premature ventricular contraction (V)," "fusion of ventricular and normal (F)," and "paced beat (Q)." For our binary classification task, we have labelled "N" as "normal" and all other categories ("S," "V," "F," "Q," etc.) as "abnormal." This binary categorization aims to simplify the initial classification challenge and focus on the robustness of the extracted features using the proposed method.

PTB Diagnostic ECG Database: This dataset comprises ECG records from 290 subjects, including 148 diagnosed with myocardial infarction (MI), 52 healthy controls, and the remaining diagnosed with other cardiac diseases. Each record contains 12-lead ECG signals sampled at 1000 Hz with 16-bit resolution. In this study, we focused on ECG lead II and used the MI (Myocardial Infarction) and healthy control categories for our analysis. We labelled "healthy control" as "normal" and "MI" along with other cardiac disorders as "abnormal." The categorization simplifies the classification objective, aligning with our focus on binary classification to validate feature extraction.

2.2. EEMD Based Decomposition

The performance measurements of EMD can be improved using ensemble mean, where data to be processed are treated as separate observations and each observation contains different noise over an ensemble of the entire signal [10]. To generalize this ensemble idea, noise is introduced to each single sequence of data. Then separate observations were indeed being made as an analogue to a physical experiment that could be repeated many times.

To establish an ensemble process possible random noise can be generated as white noise with known properties. With the help of these known characteristics of noise signal multiple observations are mimicked which is then added to each single observation. To carry out EMD on each observation of a signal, added white noises provide a uniform distribution scale of reference. Therefore, the low signal-noise ratio will not affect the decomposition method but enhances it by avoiding mode mixing. Based on this remark, an additional step is taken by arguing that adding white noise may help extract the true signals in the data, a method that is termed Ensemble Empirical Mode Decomposition (EEMD) [8, 9].

The Enhanced Empirical Mode Decomposition (EEMD) involves a systematic procedure with the following essential steps:

1. Generation of White Noise with Known Properties.
2. Addition of Noise to the Original Signal.
3. Decomposition of the Noisy Signal into Oscillatory Components.

4. Iteration for All Generated White Noise.
5. Finalize the Decomposed Signals: The ensemble mean of the corresponding intrinsic mode functions (IMFs) from all decompositions results in the finalized set of decomposed signals.

The key properties of the white noise used in EEMD are crucial to its effectiveness:

1. Even Distribution on All Timescales: The added white noise ensures a relatively uniform distribution across all timescales, contributing to a comprehensive exploration of signal characteristics.
2. Dyadic Filter Bank Property: This property imparts control over the periods of oscillations within an oscillatory component, significantly reducing the likelihood of scale mixing. Through ensemble averaging, the impact of added noise is mitigated, leading to more robust decompositions.

Fig. 1 illustrates the IMFs generated from EEMD without the application of the optimization algorithm.

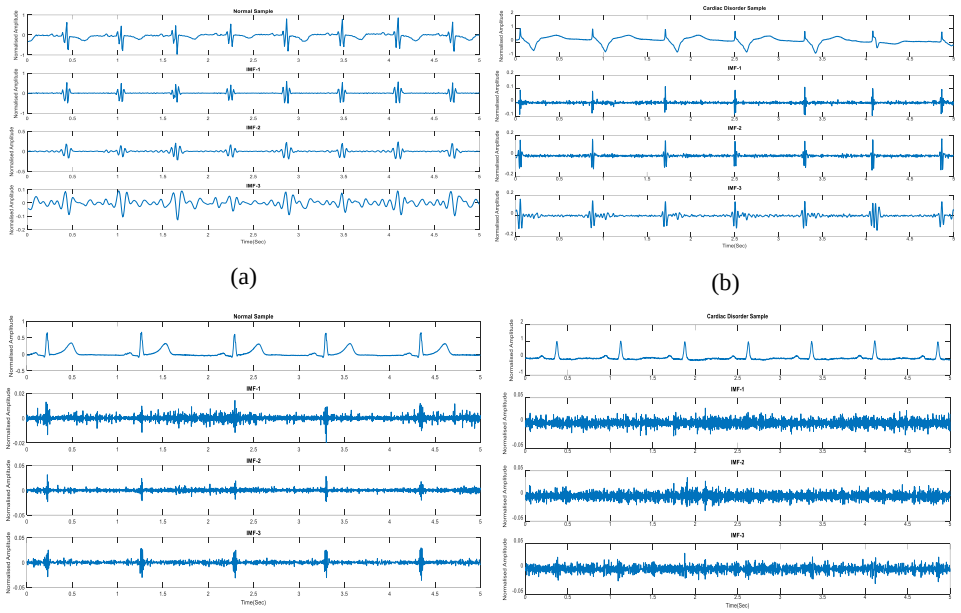

Fig. 1 Extracted IMFs without using optimization (a) Signal from the MIT-BIH Normal Sinus Rhythm Database, record no. 'nsrdb/16265', sampled at 128 Hz. (b) Signal from the MIT-BIH Arrhythmia Database, record no. 'mitdb/104', sampled at 360 Hz, representing a cardiac disorder. (c) Signal from the PTB Diagnostic ECG Database, sinus-rhythm ECG, record no. 'ptbdb/patient165/s0322lre', sampled at 1000 Hz. (d) Signal from the PTB Diagnostic ECG Database, record no. 'ptbdb/patient058/s0216lre', with a sample rate of 1000 Hz, showing a cardiac disorder.

Fig. 2 depicts the decomposition of different ECG signals into their first three IMFs using an EEMD method. Fig. 2(a) shows the IMFs for an ECG signal with atrial fibrillation, highlighting the characteristic irregularities in the waveform. The IMFs capture the erratic and disorganized electrical activity for a ventricular fibrillation ECG signal, shown in Fig. 2(b). Fig. 2(c) depicts the IMFs for an ECG signal with pauses, suggesting a stoppage in the heart's electrical activity. The IMFs of ECG signals with a normal sinus rhythm that demonstrate the regular and periodic nature of the heartbeat are shown in Fig. 2(d). These decompositions analyze the unique characteristics found in each IMF, which aids in differentiating various heart diseases.

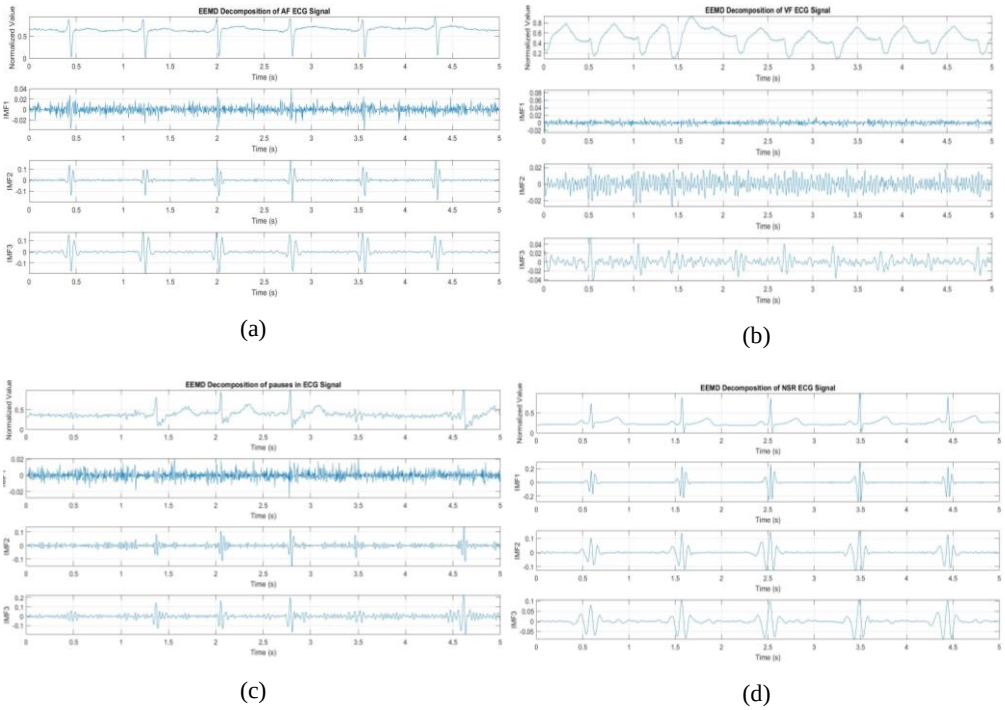

(a) (b)

(c) (d)

Fig. 2 The first three IMFs after applying EEMD to ECG signals: (a) an atrial fibrillation ECG signal from the MIT-BIH Atrial Fibrillation Database, record no. 'afdb/04126', sampled at 250 Hz; (b) a Ventricular Fibrillation ECG signal from the MIT-BIH Malignant Ventricular Ectopy Database, record no. 'vfdb/418', sampled at 250 Hz; (c) a signal with pauses from record no. '232', sampled at 360 Hz; (d) a sinus rhythm ECG signal from the MIT-BIH Normal Sinus Rhythm Database, record no. 'nsrdb/16265', sampled at 128 Hz.

2.3. Optimized EEMD IMFs

The performance of EEMD is significantly impacted by additive noise parameters like the standard deviation of white noise and the number of ensembled signals. Getting optimal values for these two parameters will best fit the EEMD and hence obtained IMFs will be better [10, 12, 16]. A robust and well-established fitness function is always of prime importance for an optimization problem.

While there are many statistical parameters like entropy and correlation, they may not perfectly represent issues of over-decomposition and under-decomposition when taken individually. To address these issues, a novel fitness function (*f*) has been proposed that reduces the error in the EEMD process. This fitness function depends upon two parameters namely correlation coefficient (C) and standard deviation (S).

$$fitness = \frac{C+S}{2} \tag{1}$$

Considering IMFs in EEMD as N scalar observations, the correlation coefficient between two IMFs at ith and jth instant is C_i^j and the maximum correlation coefficient (C) is defined as

$$C=\max\left(\{C_i^j\}\right) \tag{2}$$

Where the correlation among the IMFs can be formulated as

$$C_i^j = \frac{\sum_{t=1}^{N}[u_i(t)-\mu_{ui}][u_j(t)-\mu_{uj}]}{\sqrt{\sum_{t=1}^{N}[u_i(t)-\mu_{ui}]^2}\sqrt{\sum_{t=1}^{N}[u_j(t)-\mu_{uj}]^2}} \tag{3}$$

Where u_i and u_j represent two different IMFs with mean of μ_{ui} and μ_{uj} respectively.

The standard deviation(S) can be found from the ratio of variation of decomposed signals to the original ECG signals $x(t)$, as given in equation (4).

$$S = \sqrt{\frac{\sum_{t=1}^{N}[x(t)-\sum_{i=1}^{M}u_i(t)]^2}{N}} \tag{4}$$

The two parameters present in the developed fitness function address two major issues in signal decomposition. High correlation among decomposed signals leads to an over-decomposition problem, which restricts decomposed signals from carrying unique information. At the same time lowering this value may create a reverse issue of under decomposition. So, the other parameter in the fitness function i.e. standard deviation takes care of this problem. The lesser the value of standard deviation fewer chances will be there for under decomposition. Thus considering both leads to the generation of optimized IMFs.

2.3.1. PSO-EEMD

From many of the population-based optimization algorithms, PSO is a widely used method that searches for the best decision variable that can be represented as a surface in an n-dimensional space [17]. The philosophy behind the algorithm is each particle in the population has its position and velocity where the position represents the value of the decision variable. With each iteration, the position of the particle changes as per the velocity updating using equation (5) below:

$$v_i^{t+1} = w * v_i^t + c_1 r_1 \left(p_{best,i}^t - x_i^t\right) + c_2 r_2 \left(g_{gbest}^t - x_i^t\right) \quad (5)$$

Where
$v_i^{t+1} = Velocity\ for\ next\ iteration$
$v_i^t = Current\ velocity$
$w = Inertial\ weight$
$p_{best,i}^t = current\ personal\ best\ position\ of\ ith\ particle$
$g_{gbest}^t = current\ global\ best$
$c_1, r_1, c_2, r_2 = PSO\ initialisation\ parameters$

Once the velocity is updated it will adopt a new position using formula:

$$x_i^{t+1} = x_i^t + v_i^{t+1} \quad (6)$$

Where
$x_i^{t+1} = Next\ position (Updated\ position)$
$x_i^t = Current\ position$

There are many variants of PSO available with remarkable advantages like a derivative-free approach, less number of iterations, and ease of implementation. However, it suffers from limitations like slower convergence and huge computational time making it restricted to certain applications.

In our work, we used PSO to return optimized values of decision variables using the fitness function equation (1).

2.3.2. WOA-EEMD

The special hunting behaviour of humpback whales popularly known as the bubble net feeding method makes it suitable for many optimization problems [11]. These whales usually target small fishes close to the surface. Earlier it was assumed that two manoeuvres are associated with bubbles and named them ‘upward-spirals’ and ‘double-loops’. To do so humpback whales dive around 12 m down and then start to create a bubble in a spiral shape around the prey and swim up towards the surface. Goldbogen et al. found three different stages for optimization: coral loop, lobtail, and capture loop [18]. Detailed information about these behaviours can be found in [11]. It is worth mentioning here that bubble-net feeding is a unique behaviour that can only be observed in humpback whales. Mathematically, it can be modeled as:

$$D = |C.X^*(t) - X(t)| \quad (7)$$

$$X(t+1) = X^*(t) - A.D \quad (8)$$

Where

$$A = 2\,a.r - a \quad (9)$$

$$C = 2.r \quad (10)$$

$$X(t+1) = \begin{cases} X^*(t) - A.D \\ D.e^{bl}.\cos(2\pi l) + X^*(t) \end{cases} \quad (11)$$

Pseudo code for whale optimization algorithm is represented as:

```
1. Initiate Population
2. Calculate the fitness of each search agent
        3. X*=best whale (the whale with the best fitness)
4. While (terminating condition not met)
  For each whale (search agent):
     Update control parameters a, A, C, l, P
        If(P<0.5):
              If abs(A)<1
                    Update the position using Eq. (8)
              Else:
                    Select a random whale
                    Update position using Eg. (11-b)
              Endif
          Else:
              Update position using Eg. (11-a)
         Endif
    End for
    Update X* if a better whale is found
5. End While
6. Return X* (the optimal solution)
```

2.4. Optimization Parameters

Some initialisation parameters for the optimization methods considered are taken based on some experiments carried out and summarized in below table.

Table 1 Description of parameters for the optimization algorithm

Optimization Technique	Parameter
Particle Swarm Optimization	Maximum Iterations:50 C1:1.2 C2:2.4 No. of Particles:50
Whale Optimization Algorithm	Maximum Iterations:50 Population:50 r: random a:2~0(linearly decreasing)

Fig. 3 represents the IMFs extracted using PSO-EEMD for a sample from both normal sinus rhythm and cardiac disorder signals.

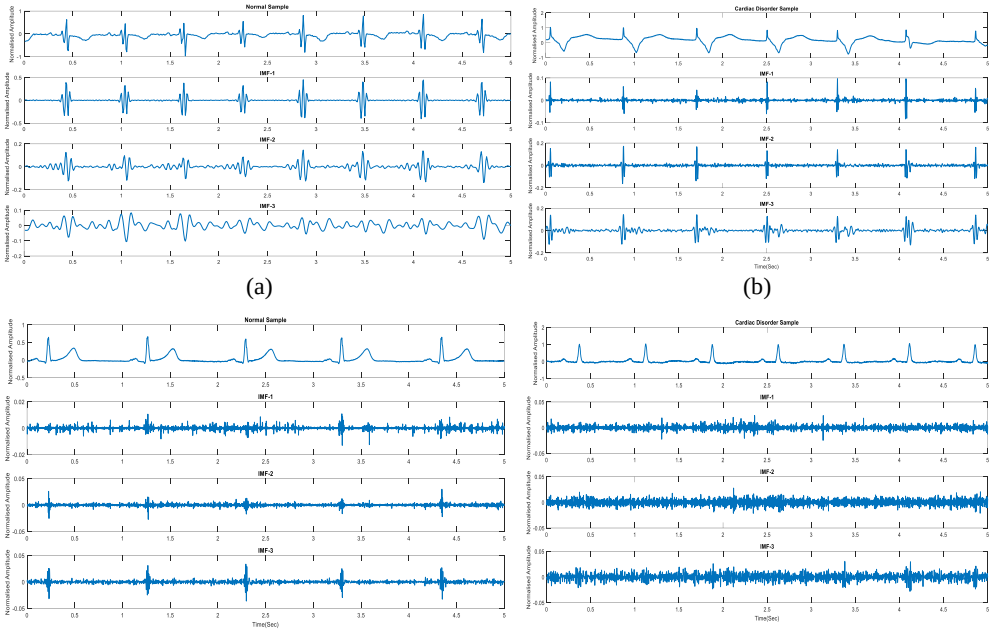

Fig. 3 Extracted IMFs using optimization (a) Signal from the MIT-BIH Normal Sinus Rhythm Database, record no. 'nsrdb/16265', sampled at 128 Hz. (b) Signal from the MIT-BIH Arrhythmia Database, record no. 'mitdb/104', sampled at 360 Hz, representing a cardiac disorder. (c) Signal from the PTB Diagnostic ECG Database, sinus-rhythm ECG, record no. 'ptbdb/patient165/s0322lre', sampled at 1000 Hz. (d) Signal from the PTB Diagnostic ECG Database, record no. 'ptbdb/patient058/s0216lre', with a sample rate of 1000 Hz, showing a cardiac disorder.

2.5. Optimized Features

In our work to get the best possible features or optimized features, we need to have better IMFs extracted from ECG signals. So, to accomplish this instead of finding optimized features directly we obtained optimized IMFs as stated in the previous section. Now in this section, we are going to demonstrate the way of finding features from optimized IMFs.

The analytic intrinsic mode function (IMF) is calculated by applying the Hilbert transform on all IMFs obtained by the optimized-EEMD method. For each IMF component, the analytic signal amplitude A(t) and instantaneous phase ∅(t) can be calculated to obtain the analytic IMF z(t).

Calculation of AM and FM Bandwidths:

The frequency components of a signal can be well represented by its bandwidth. Only considering the frequency spectrum, will not provide information about the amplitude or envelope of a signal [19]. Instead spread of frequencies because of deviation from mean frequency or because of change in amplitude or even both considered at a time is more informative. In [20, 21], the authors come up with a method for the calculation of two different bandwidth parameters, known as amplitude modulation bandwidth (B_{AM}) and

frequency modulation bandwidth (B_{FM}). In this study, we use B_{AM} and B_{FM} to extract important features from ECG signals. These features are important for distinguishing between normal sinus rhythm and cardiac disorders. Unlike traditional frequency spectrum analysis which mainly looks at frequency content B_{AM} and B_{FM} consider both amplitude and frequency changes. This provides a more comprehensive understanding of the signal. Both B_{AM} and B_{FM} provide critical insights into the modulation properties of the ECG signal. B_{AM} values increase when the signal exhibits significant amplitude variations, often observed in cardiac disorders ECG patterns. On the other hand, $_{BFM}$ helps in identifying frequency shifts, which can be indicative of irregularities associated with various cardiac conditions.

A well-established mathematical relation between signal and frequency components is demonstrated below where the centre frequency of analytic IMF z(t) is given by

$$\langle w \rangle = \frac{1}{E} \int w |Z(w)|^2 dw \tag{12}$$

In the above equation E is the energy of signal z(t), and Z(w) is the Fourier transform of signal z(t).

Equation (12) can also be represented as

$$\langle w \rangle = \frac{1}{E} \int z^*(t) \frac{1}{j} \frac{dz(t)}{dt} dt \tag{13}$$

Considering each component of z(t) in (13), the expression in (13) can be further expressed as

$$\langle w \rangle = \frac{1}{E} \int \left(\frac{d\emptyset(t)}{dt} - \frac{j}{A(t)} \frac{dA(t)}{dt} \right) A^2(t) dt \tag{14}$$

The second term is zero since that term is purely imaginary, it must be zero for center frequency $\langle \omega \rangle$ to be real quantity. Therefore, the center frequency is given by

$$\langle w \rangle = \frac{1}{E} \int \frac{d\emptyset(t)}{dt} A^2(t) dt \tag{15}$$

The bandwidth of the analytic IMF z(t) can be defined as

$$B^2 = \frac{1}{E} \int (w - \langle w \rangle)^2 |Z(w)|^2 dw \tag{16}$$

Equation (16) can be expressed as

$$B^2 = \frac{1}{E} \int \left| \left(\frac{1}{j} \frac{d}{dt} - \langle w \rangle \right) z(t) \right|^2 dt \tag{17}$$

Substituting z(t) from (16) into (17), the expression in (17) can be further expressed as

$$B^2 = \frac{1}{E} \int \left(\frac{dA(t)}{dt} \right)^2 dt + \frac{1}{E} \int \left(\frac{d\emptyset(t)}{dt} - \langle w \rangle \right)^2 A^2(t)\, dt \tag{18}$$

It is clear that the bandwidth of the signal has two terms, one depending on the amplitude and the other depending only on the phase. Therefore, two features from each decomposed signal in terms of bandwidth due to amplitude modulation (B_{AM}) and the bandwidth due to frequency modulation (B_{FM}) are defined as

$$B_{AM}^2 = \frac{1}{E} \int \left(\frac{dA(t)}{dt} \right)^2 dt \tag{19}$$

$$B_{FM}^2 = \frac{1}{E}\int \left(\frac{d\emptyset(t)}{dt} - \langle w \rangle\right)^2 A^2(t)\, dt \tag{20}$$

As shown in the fig. 4 till the terminating condition is reached the decision variables go on changing and once converged results are obtained, we calculated IMFs. These IMFs are then used for calculating AM/FM bandwidths to be considered as features.

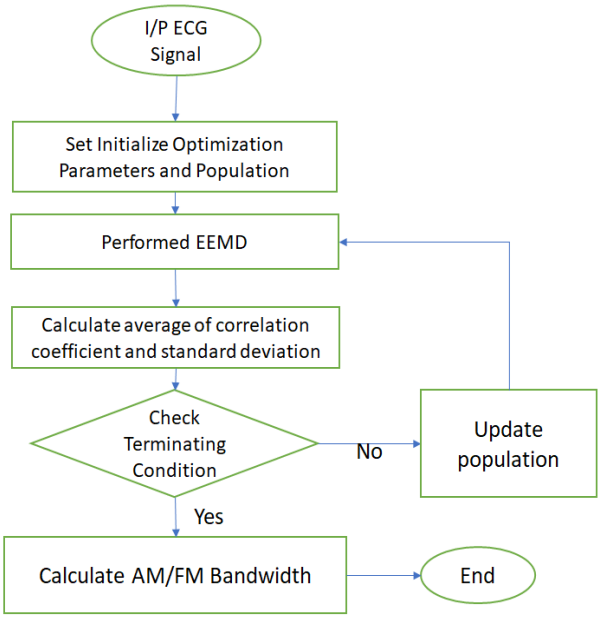

Fig. 4 Flowchart of the proposed optimized EEMD-based AM/FM bandwidth feature extraction

2.6. Feature Extraction Using EEMD

We use important features like frequency modulation bandwidth (B_{FM}) and amplitude modulation bandwidth (B_{AM}) derived from the intrinsic mode functions (IMFs) obtained by the EEMD process to identify anomalies in ECG data.

Amplitude Modulation Bandwidth (B_{AM}): B_{AM} of an IMF represents the range of amplitude fluctuations within it. Arrhythmias and other irregularities in the ECG signal cause irregular amplitude variations, which increase B_{AM}. For instance, atrial fibrillation causes the amplitude variations to become more irregular, as shown by an increased B_{AM}. This indicate the existence of an irregular rhythm.

Frequency Modulation Bandwidth (B_{FM}): B_{FM} measures the frequency range in which the signal oscillates. Irregular heartbeats have increased B_{FM} and fluctuate in frequency, whereas regular heartbeats have a consistent rhythm. For example, ventricular fibrillation causes rapid, irregular heartbeats, which results in a broader B_{FM} and indicates the presence of a cardiac disorder.

The ECG signal is decomposed into IMFs using the EEMD method, from which B_{AM} and B_{FM} are obtained. These features provide classifiers like Support Vector Machines and Decision Trees to help distinguish between sinus-rhythm ECG and cardiac disorders ECG signals. These features' effectiveness is evaluated by classification accuracy, which demonstrates their utility in diagnosing abnormalities.

Typical B_{AM} and B_{FM} values for various ECG signals are shown in Table 2. These values, derived from the first three IMFs of ECG signals in the PTBDB and MIT-BIH databases, are the most important for describing ECG signals. B_{AM} and B_{FM} values in normal ECG signals are generally steady within a specific range. On the other hand, cardiac disorder ECG signals exhibit greater fluctuation in these values, indicating underlying cardiac issues.

Table 2 Bandwidth Features of the IMFs for sinus-rhythm ECG and cardiac disorders ECG Signals

Database	Signal Type	B_{AM} ($\times 10^3$ Hz)			B_{FM} (Hz)		
		IMF1	IMF2	IMF3	IMF1	IMF2	IMF3
PTB-DB	Sinus-rhythm ECG	2.7458	2.5859	2.3925	195.042	130.0147	179.8747
	Cardiac disorders ECG	3.9992	2.2205	1.8627	254.3380	230.9884	164.7964
MIT-BIH	Sinus-rhythm ECG	2.25966	2.315662	2.253651	201.8384	206.8406	201.3016
	Cardiac disorders ECG	1.908506	3.423781	3.336431	170.4724	305.8205	298.0181

The first three IMFs in both datasets have the same B_{AM} and B_{FM} values for sinus-rhythm ECG signals. However, cardiac disorder ECG signals show noticeable increases in B_{AM} and B_{FM} values in comparison to normal sinus rhythm signals. This increase reflects the greater complexity and irregularity of the signal caused by arrhythmias such as atrial fibrillation and ventricular fibrillation. The results demonstrate that cardiac disorder ECG signals, especially when arrhythmias are present, exhibited higher B_{AM} and B_{FM} values. These features are essential for differentiating between sinus-rhythm and cardiac disorders events, which builds the foundation for accurately classifying and diagnosing cardiac diseases.

3. Results and Discussion

The best utilisation of search space by any of the optimization algorithms makes it efficient not just in finding the optimal solution but also in getting those values in a quick time. Keeping these things, the prime objective is to enhance the outcome of EEMD with the application of two nature-inspired population-based optimization algorithms, below are the results obtained. Very appreciable work done by WOA is its quick convergence strategy and also it getting reflected in our application, which resulted in a convergent outcome in just 15~20 iterations as compared to 35~45 iterations for PSO.

3.1. Optimization Case Study

As stated, two population-based bio-inspired optimization techniques are considered for the analysis of the impact of convergence and minimum cost value. The below figure shows the path of convergence for the two optimization algorithms PSO and WOA.

In Fig. 5(a) and (b), it is evident that the proposed WOA-EEMD-DT is performing well with respect to error convergence for both datasets. The primary objective of using WOA has been realized with a quick convergence from the 22nd iteration as shown in figure 5(a) for the MIT-BIH dataset and at the same time for the PTB dataset it converges from the 17th iteration shown in Fig. 4(b). Whereas in the case of PSO it converges from 35th and 47th iterations for the MIT-BIH and PTB datasets, respectively. Considering this fact, a state-forward comparison has been made with the optimized EEMD and is discussed below sections.

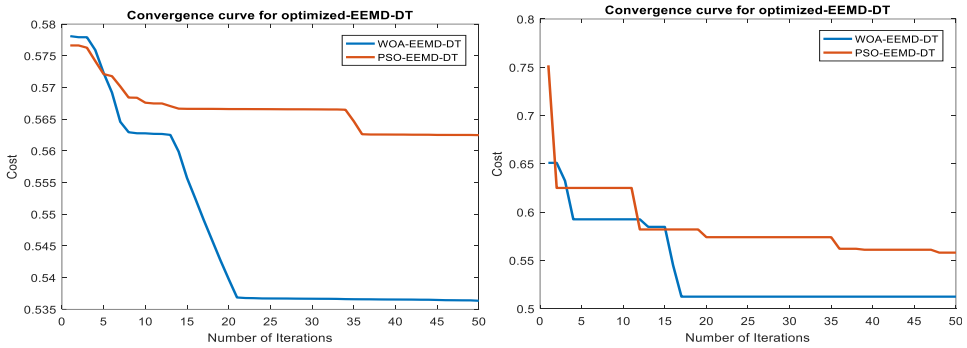

(a) (b)

Fig. 5 The Convergence curve

Evaluation Criteria:

To assess the effectiveness of the optimized feature extraction technique, we evaluated the DT and SVM classifiers using five standard criteria: accuracy (Acc), precision (Pr), recall (Re), F-score and sensitivity (Sp). These criteria are defined as follows:

$$Acc = \frac{TP + TN}{TP + TN + FP + FN} \times 100 \tag{21}$$

$$Pr = \frac{TP}{TP + FP} \times 100 \tag{22}$$

$$Re = \frac{TP}{TP + FN} \times 100 \tag{23}$$

$$F - score = 2 \times \frac{Pr \times Re}{Pr + Re} \tag{24}$$

$$Sp = \frac{TN}{TN + FP} \times 100 \tag{25}$$

Where TP and TN denote the total number of correctly identified true positive and true negative events, respectively. Conversely, FP and FN refer to the number of incorrectly identified positive and negative events, respectively.

3.1.1. PSO- EEMD

In Fig. 6(a), we present a performance comparison of the classifiers under consideration, in addition to EEMD and PSO-EEMD. It clearly shows remarkable progress in the performance of PSO-EEMD-DT as compared to EEMD-DT. Similarly, Fig. 6(b) shows enhanced performances for PSO-EEMD-SVM as compared to EEMD-SVM while processing the MIT-BIH dataset.

The performances can be analyzed even better from the values expressing the importance of PSO-EEMD over simple EEMD all performance measures. With an accuracy of 86%, PSO-EEMD depicts a good feature extraction process as compared to 80% in the case of simple EEMD. The performance measures shown here are to show the improvisation in result without proper pre-processing and an improvement of 6% is considered better here.

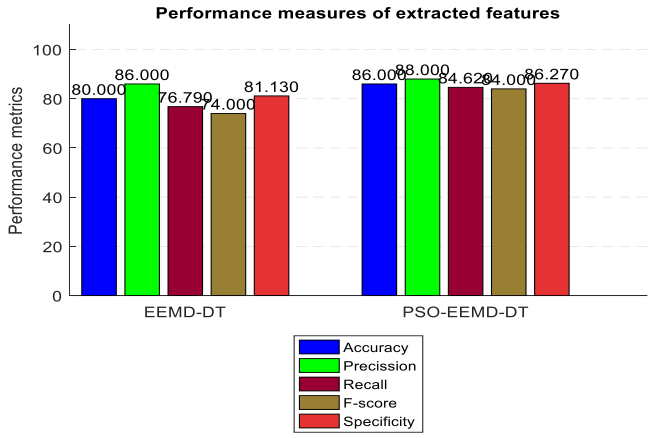

(a)

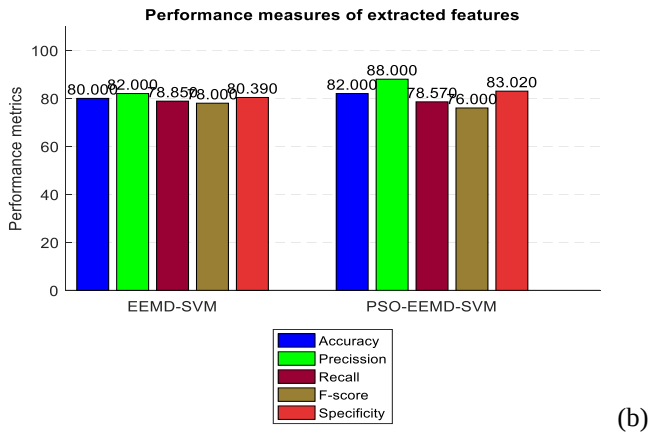

(b)

Fig. 6 The performance measure for PSO-EEMD (a) for DT classifier (b) for SVM classifier on MIT-BIH dataset

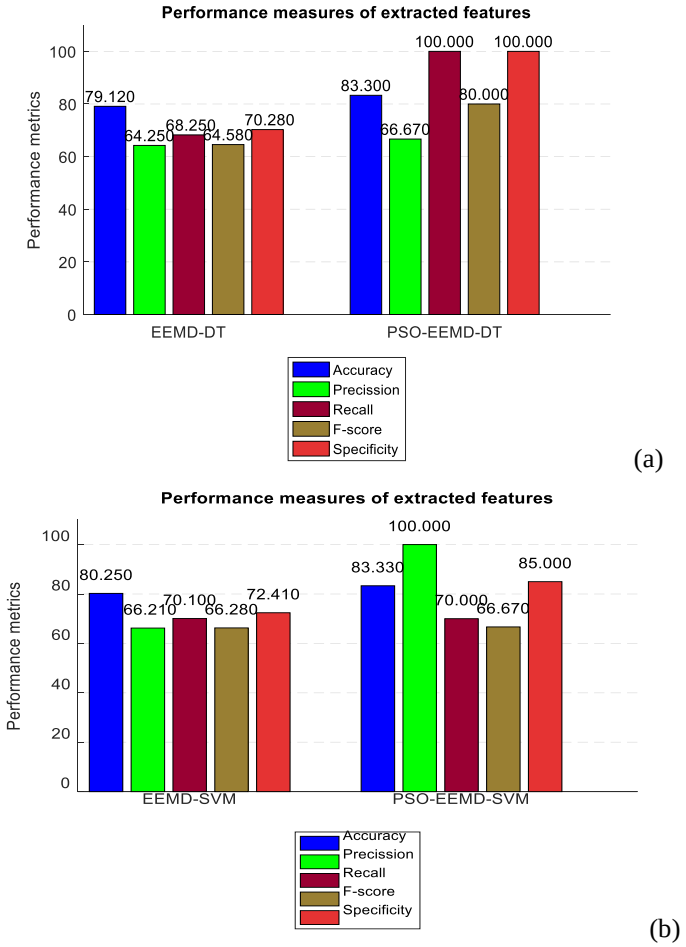

Fig. 7 Performance measure for PSO-EEMD (a) for DT classifier (b) for SVM classifier on PTB dataset

Similarly, Figure 7(a) represents the performance comparison of both the classifiers considered along with EEMD and PSO-EEMD. The performances for the PTB dataset also show better results for PSO-EEMD than in the case of MIT-BIH. It also has been shown that PSO-EEMD outperforms simple EEMD while considering features for both the classifiers showing an accuracy level of 83.3%.

3.1.2. EEMD-WOA

To check the impact of advanced bio-inspired optimization techniques, further analysis has been done using the whale optimization algorithm (WOA).

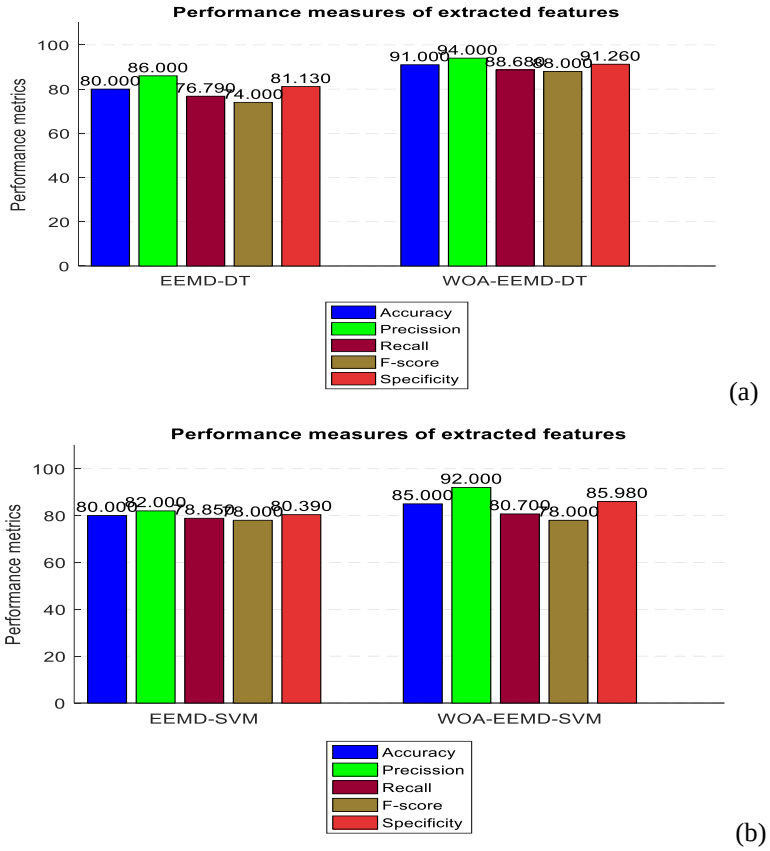

Fig. 8 The performance measure for WOA-EEMD (a) for DT classifier (b) for SVM classifier on MIT-BIH dataset

The performance of the spiral tracking path of the whale optimization algorithm not only shows better performance measures and ensures quick convergence compared to improved time complexity. Fig. 8 (a) shows better performance for the DT classifier as compared to SVM with the WOA algorithm shown in Fig. 8 (b) for the MIT-BIH dataset.

Fig. 9 further highlights the advantage of WOA-EEMD-DT. It achieves 100% accuracy compared to WOA-EEMD-SVM's 66.67%.

3.2. Comparison of PSO-EEMD and WOA-EEMD

A comparative analysis of PSO-EEMD and WOA-EEMD reveals that the fast-converging nature of WOA helps achieve better performance in shorter execution times. This suggests that the limitation of using optimization in terms of time complexity can be mitigated with a more efficient optimization technique like WOA.

Table 3 reflects the improvement in different performance measures when using WOA with the MIT-BIH dataset. WOA algorithm-based DT and SVM classifiers outperform those using PSO-optimized EEMD. As shown in Figure 7(a), the results are consistently better with WOA-EEMD compared to PSO-EEMD, achieving an accuracy level of 91%.

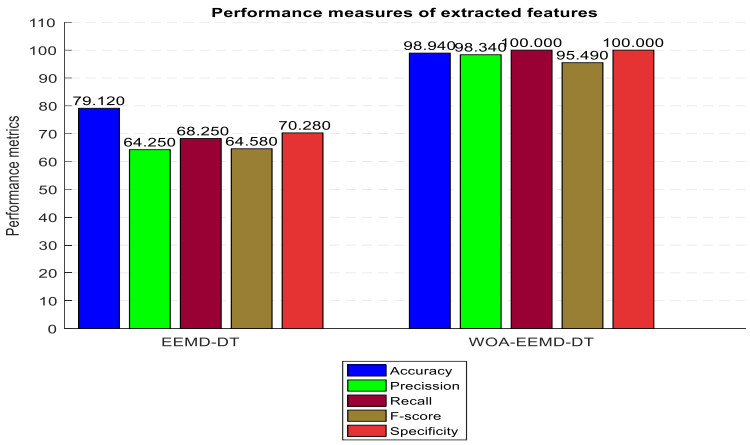

(a)

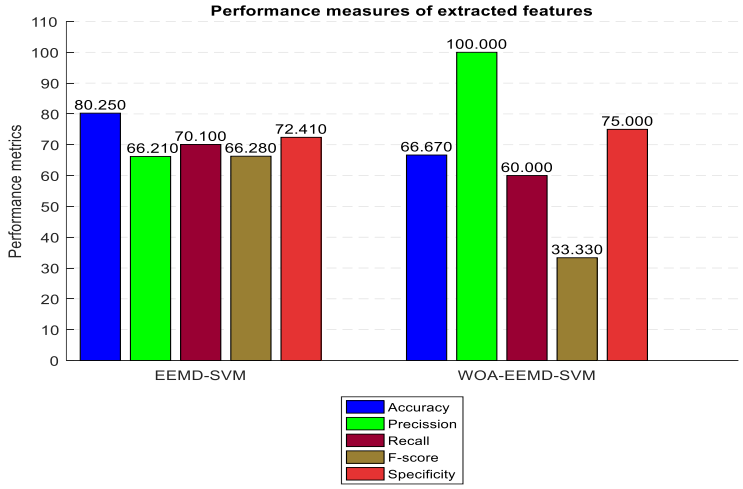

(b)

Fig. 9 Performance measure for WOA-EEMD (a) for DT classifier (b) for SVM classifier on PTB dataset

Table 3 Performance comparison of PSO-EEMD and WOA-EEMD for MIT-BIH dataset

	PSO-EEMD		WOA-EEMD	
	Decision Tree (%)	SVM(%)	Decision Tree (%)	SVM(%)
Accuracy	86	82	91	85
Precision	88	88	94	92
Recall	84.62	78.57	88.68	80.7
F-score	84	76	88	78
Specificity	86.20	83.02	91.26	85.98

Table 4 shows the improvisation while using WOA for the PTB dataset. And it very effectively shows the same improvisation as in the case of the MIT-BIH dataset. This leads to the establishment of WOA-EEMD-DT as the best-proposed approach.

Table 4 Performance comparison of PSO-EEMD and WOA-EEMD for PTB dataset

	PSO-EEMD		WOA-EEMD	
	Decision Tree(%)	SVM(%)	Decision Tree(%)	SVM(%)
Accuracy	83.33	83.33	98.94	66.67
Precision	67	100	98.34	100
Recall	100	70	100	60
F-score	80	66.67	95.49	33
Specificity	100	85	100	75

4. CONCLUSION

In conclusion, this study demonstrates the efficacy of optimized EEMD for enhanced ECG signal analysis. Key achievements include devising a fitness function to improve EEMD consistency, employing bio-inspired optimization for robust decomposition, and proposing a novel feature extraction approach that distinguishes amplitude and frequency modulation characteristics. The EMD technique has already proven effective in handling the complex information within ECG signals. This work enhances EMD by exploring hidden hyperparameters in EEMD and optimizing them over a large search space to strengthen the decomposition process. Our approach verifies that EEMD decomposition performs better with specific noise used for the ensemble.

Furthermore, we obtained that using the optimized EEMD feature extraction technique can achieve an improved accuracy of +6% compared to simple EEMD. The process can further be improvised with better machine learning and deep learning classifiers. In our work, we focused on the initial step of dealing with ECG signals rather than the classifiers. Still, without using any of the pre-processing steps we achieved an accuracy level of 91% and 98.94% for the MIT-BIH and PTB datasets, respectively. Significant improvements in the specificity of 91.26% and 100% are also recorded for MIT-BIH and PTB datasets, respectively. This indicates that selecting more robust classifiers and an advanced optimization strategy for the developed objective function can yield even better results.

Overall, this study significantly advances ECG analysis by enhancing decomposition reliability. The presented framework helps mitigate perturbations while retaining modulation characteristics essential for pathophysiological insights. Future efforts will focus on translating these methods for automated annotation of cardiac disorder beats and infarction detection, thereby assisting clinicians through intelligent ECG interpretation.

REFERENCES

[1] L. Holmstrom, H. Chugh, K. Nakamura, et al., "An ECG-based artificial intelligence model for assessment of sudden cardiac death risk", *Commun. Med.*, vol. 4, p. 17, 2024.

[2] M. Hassaballah, Y.M. Wazery, I.E. Ibrahim, A. Farag, "ECG Heartbeat Classification Using Machine Learning and Metaheuristic Optimization for Smart Healthcare Systems", *Bioengineering*, vol. 10, no. 4, p. 429, 2023.

[3] C. Satheesh Pandian, A. M. Kalpana, "HybDeepNet: ECG Signal Based Cardiac Arrhythmia Diagnosis Using a Hybrid Deep Learning Model", *Information Technology and Control*, vol. 52, no. 2, pp. 416–432, 2023.
[4] R. Saravana Ram, J. Akilandeswari, M. Vinoth Kumar, "HybDeepNet: A Hybrid Deep Learning Model for Detecting Cardiac Arrhythmia from ECG Signals", *Information Technology and Control*, vol. 52, no. 2, p. 433–444, 2023.
[5] T.Y. Hou, M.P. Yan, Z. Wu, "A variant of the EMD method for multi-scale data", Advances in Adaptive Data Analysis, vol. 1, no. 4, pp. 483–516, 2009.
[6] G. Jager, R. Koch, A. Kunoth, R. Pabel, "Fast Empirical Mode Decompositions of multivariate data based on adaptive spline-wavelets and a generalization of the Hilbert–Huang-transform (HHT) to arbitrary space dimensions", *Advances in Adaptive Data Analysis*, vol. 2, no. 3, pp. 337–358, 2010.
[7] G. Rilling, P. Flandrin and P. Goncalves, "On empirical mode decomposition and its algorithms", In Proceedings of the IEEE-EURASIP Workshop Nonlinear Signal Image Process, 2003, pp. 8–11.
[8] K. Polat and S. Gunes, "Classification of epileptiform EEG using a hybrid system based on decision tree classifier and fast Fourier transform", *Applied Mathematics and Computation*, vol. 187, no. 2, pp. 1017–1026, 2007.
[9] T. Y. Hou, Z. Shi, "Data-driven time–frequency analysis. Applied and Computational Harmonic Analysis", vol. 35, no. 2, pp. 284–308, 2013.
[10] Z. WU, & N. E. HUANG, "Ensemble Empirical Mode Decomposition: A Noise-Assisted Data Analysis Method", *Advances in Adaptive Data Analysis*, vol. 01, no. 01, pp. 1–41, 2009.
[11] S. Mirjalili and A. Lewis, "The Whale Optimization Algorithm", Advances in Engineering Software 95, pp. 51–67, 2016.
[12] El-Ghazali Talbi, Metaheuristics: From Design to Implementation, John Wiley & Sons, 2009.
[13] J. Kennedy and R. Eberhart, "Particle swarm optimization", In Proceedings of ICNN'95 - International Conference on Neural Networks, Perth, WA, Australia, 1995, vol.4, pp. 1942–1948.
[14] A.L. Goldberger, L. A. Amaral, L. Glass, J. M. Hausdorff, P. C. Ivanov, R. G. Mark, J. E. Mietus, G. B. Moody, C. K. Peng, H. E. Stanley, PhysioBank, PhysioToolkit, and PhysioNet: Components of a "New Research Resource for Complex Physiologic Signals", *Circulation*, vol. 101, pp. 215–220, 2000.
[15] A. for the Advancement of Medical Instrumentation et al., "Testing and Reporting Performance Results of Cardiac Rhythm and ST-segment Measurement Algorithms", The Association, ANSI/AAMI EC38, 1999.
[16] P. Dehkordi, A. Garde, B. Molavi, J. M. Ansermino, & G. A. Dumont "Extracting Instantaneous Respiratory Rate From Multiple Photoplethysmogram Respiratory-Induced Variations", *Frontiers in Physiology*, vol. 9, pp. 1–10, 2018.
[17] A. Garde, W. Karlen, P. Dehkordi, J. Ansermino and G. Dumont, "Empirical mode decomposition for respiratory and heart rate estimation from the photoplethysmogram", *Computing in Cardiology*, pp. 799–802, 2013.
[18] J.A. Goldbogen, A.S. Friedlaender, J. Calambokidis, M.F. Mckenna, M. Simon, D.P. Nowacek, "Integrative approaches to the study of baleen whale diving behavior, feeding performance, and foraging ecology", *BioScience*, vol. 63, no. 2, pp. 90–100, 2013.
[19] H. Ye, J. Zhu, Y. Cheng, D. Xue, B. Wang, & Y. Peng, "PPG based Respiration Signal Estimation using VMDPCA", In Proceedings of the 24th International Conference on Automation and Computing (ICAC), 2018, pp. 1–5.
[20] B. van der Pol. "The fundamental principles of frequency modulation Part III: Radio and Communication Engineering", *J. Inst. Electr. Eng.*, vol. 93, pp. 153–158, 1946.
[21] G. Rilling and P. Flandrin, "One or Two Frequencies? The Empirical Mode Decomposition Answers", *IEEE Transactions on Signal Processing*, vol. 56, no. 1, pp. 85–95, 2008.